

Exploring Equilibrium Points in a Long-term Glucose-insulin Model for Type I Diabetes: MPC Application in Automated Insulin Delivery Systems Using Functional Insulin Therapy Tools

Amor Hamata^{1*}, Salim Aissi²

¹Laboratory of Advanced Electronics,
Electronics Department,
University of Batna 2, Mostafa Benboulaïd, Algeria
E-mail: a.hamata@univ-batna2.dz

²Laboratory of Advanced Automation and Analysis Systems,
Electronics Department,
University of Batna 2, Mostafa Benboulaïd, Algeria
E-mail: s.aissi@univ-batna2.dz

*Corresponding author

Received: March 11, 2024

Accepted: July 01, 2024

Published: March 31, 2025

Abstract: This study explores a novel approach to regulate blood glucose levels in individuals with type I diabetes, employing the widely used model predictive control (MPC) strategy in type I diabetes mellitus therapy and clinical trials. The MPC algorithm is implemented based on Magdelaine's long-term glucose-insulin model, which encompasses real-life characteristics often absent in other prevalent models. The control strategy is evaluated through simulations involving 10 virtual patients from existing literature. The simulations encompass fasting scenarios and a closed-loop control scenario involving three meals. MPC results are compared to those of the "optimal" conventional insulin daily injections therapy (open-loop treatment), especially under "aggressive conditions" including elevated initial blood glucose levels, substantial carbohydrate intake, closely spaced meal times, and incorporating a time delay between plasma glucose concentration and its subcutaneous measurement. The MPC algorithm demonstrated remarkable efficacy in glycemic control for 80% of patients, achieving an average time-in-range percentage exceeding 80% with no hypoglycemic episodes. This aligns with the American Diabetes Association's recommendation of spending at least 70% of the time in the target range for effective glycemic control and maintaining an average time spent in hypoglycemia of less than 4%. However, the same MPC controller exhibited suboptimal performance for two patients, with an average time spent in hypoglycemia exceeding 8%. These findings underscore the need for individualized adjustments of MPC parameters or alternative control strategies to optimize glycemic management in all patients.

Keywords: Type I diabetes, Equilibrium points, Open-loop therapy, Closed-loop control therapy, Model predictive control, Functional insulin therapy tools, Time in range.

Introduction

The type 1 diabetes (T1D) is a chronic autoimmune disease that causes an irreversible destruction of the beta cells. In such conditions the pancreas can't secrete insulin and the blood glucose is no longer regulated [1]. The actual treatment consists of exogenous insulin injections, adapted to the organism's needs. It can be given as many daily injections or it can be delivered by an insulin pump that uses both programmed continuous subcutaneous insulin infusion and pre-prandial boluses. In each case, the objective is to maintain glucose levels within a safe range between 70 and 180 mg/dl, commonly referred to as euglycemia, defined in the

literature as time in range (TIR) [2, 12, 16, 22, 26, 31, 33]. If the injected doses are underestimated, blood sugar levels may accumulate, leading to hyperglycemia (glucose levels above 180 mg/dl), also known as time above range (TAR). Conversely, if the insulin doses are significantly elevated, blood glucose levels sharply decrease, resulting in hypoglycemia with values below 70 mg/dl, termed time below range (TBR). Clinical protocols are employed to improve the accuracy of estimating the required insulin injections for a patient. In this context, functional insulin therapy (FIT) is an educational program designed to assist the patient in calculating insulin doses. The knowledge of the FIT parameters is important for medical professionals. The scientific community often overlooks these parameters when developing new models for insulin-glucose dynamics in type 1 diabetes cases. Well-defined FIT parameters would facilitate the evaluation of mathematical models and consequently, enhance control over disturbances [30].

FIT defines tools such as insulin sensitivity factor (ISF), also known as correction factor (CF) and carbohydrate to insulin ratio (CIR). These tools are used to calculate insulin boluses based on factors such as blood glucose (BG) level, BG target, meal carbohydrate (CHO) content, and the insulin on board (IOB) remaining from previous boluses [24]. Another highly significant tool is the basal rate. It's the amount of insulin that must be continuously present in the bloodstream to ensure the availability of glucose. Basal insulin dose determination is the key to successful flexible insulin therapy [3].

All glycaemic targets should be individualised and agreed with the person with diabetes. Lower or higher targets may be appropriate according to individual characteristics [16]. The intersubject variability characterizing the patients affected by type 1 diabetes mellitus (T1DM) makes automatic blood glucose control very challenging. Different patients have different insulin responses and control law based on a non-individualized model could be ineffective. FIT aims at personalizing the treatment provided to each individual patient based on sensitivity factors that enable the quantification of specific exogenous insulin needs in response to specific external disturbance inputs (i.e. carbohydrates, stress or physical activity) [30]. A linear individualized glucose-insulin model has demonstrated promising potential in designing personalized control algorithms for blood glucose level regulation [23].

The need of the hour for medical professionals is the dependable and efficient automation of biomedical therapies. In recent years, model predictive control (MPC) strategy has been widely used in T1DM therapy and clinical trials, more than proportional integral derivative (PID) and fuzzy logic [26]. Intelligent techniques such as artificial neural networks and metaheuristic algorithms [29] are frequently used. The backstepping technique [13] and robust H_∞ control have also been used in some studies [7, 8, 14, 15, 17-21, 25, 27, 28, 35-37].

The automated insulin delivery system

The prospect of a biological cure for type 1 diabetes in the near future is not feasible [11, 14, 15, 23, 30, 32, 38]. Nonetheless, advancements in diabetes management have led to the development of “technical” solutions, such as automated insulin delivery (AID) systems [17]. These AID systems integrate data from a continuous glucose monitoring (CGM) system, a control algorithm, and an insulin pump to automate subcutaneous insulin delivery [32]. The decision of how much insulin to infuse with insulin pump is made by the control algorithm. In general, this algorithm is based on a mathematical model that is required to suitably describe the insulin-glucose dynamics. Thus, the model constitutes a key element in the development of a reliable AID. AID systems have started to become widely used by a new population of patients with type 1 diabetes to mimic natural insulin production [2, 7-12, 14-23, 25-38]. Since the first

model proposed by Bolie in 1961 [6], the dynamics of blood sugar and insulin have been modeled many times. Most of these models have been established and validated using glucose tolerance test data from non-diabetics or type 2 diabetics. Later on, adaptations were made to model type 1 diabetes, resulting in three notable nonlinear models: Bergman minimal model, Hovorka model and Dalla man model (the only UVA/Padova simulator approved by the U.S. Food and Drug Administration is based on the Dalla man’s model). These models have become prominent landmarks in the field of diabetes research and clinical practice. However, the calculation of the equilibrium points of these models during fasting has shown that any constant basal insulin rate maintains constant glycemia at a value depending on this rate [19]. As with the latter models, any constant basal insulin rate regulates blood sugar. Consequently, in a dynamic regime, the glycemia after a meal not accompanied by a bolus would reach the equilibrium value fixed by the constant infused rate as shown in Fig. 1. However, this behavior contradicts clinical observations, making it a significant drawback of their approach.

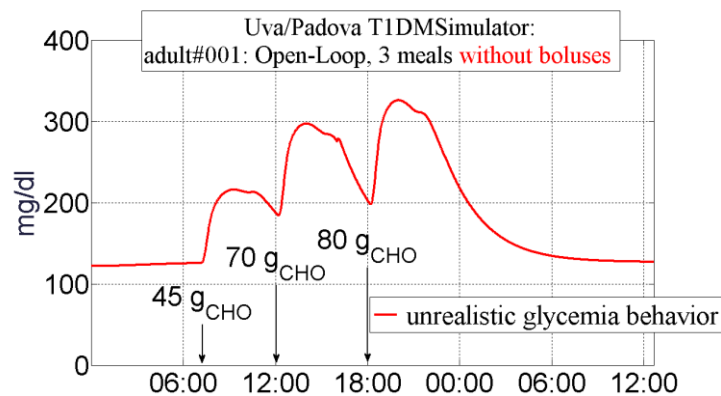


Fig. 1 UVA/Padova simulator: open-loop virtual patient response for three meals without boluses [21]

An unrealistic equilibrium point can have diverse effects on the system’s dynamics, including inaccurate predictions, artificial stability or instability, incompatibility with empirical observations. These potential impacts highlight the importance of establishing realistic equilibrium points for more accurate understanding and representation of a system’s behavior.

Materials and methods

Magdelaine’s long-term glucose-insulin linear model

The Magdelaine’s linear model consists of three main dynamics with five ordinary differential equations, as shown in Fig. 2 and Fig. 3. The insulin diffusion dynamics are represented using a two-compartment subsystem comprising a subcutaneous compartment and a blood plasma compartment. Similarly, the digestion subsystem, encompassing the stomach and the duodenum, is also modeled with a two-compartment approach. These second-order models are selected to align with the pharmacokinetics of insulin and the appearance rate of glucose in the blood plasma after a meal.

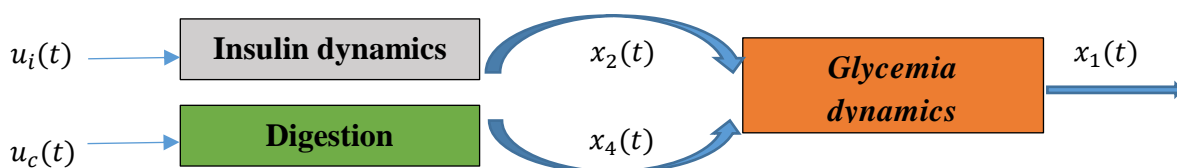


Fig. 2 Model structure

The model consists also two inputs, namely the insulin injection rate u_i , [U/min], the carbohydrate ingestion rate u_c , [g/min], and one output, which is the blood glucose concentration x_1 , [mg/dl]. The state variable x_2 is the plasma insulin flow, [U/min], x_3 is the insulin flow in the subcutaneous compartment, [U/min], x_4 represents the carbohydrate flow in the duodenum, [g/min], and x_5 is the carbohydrate flow in the stomach, [g/min] [19].

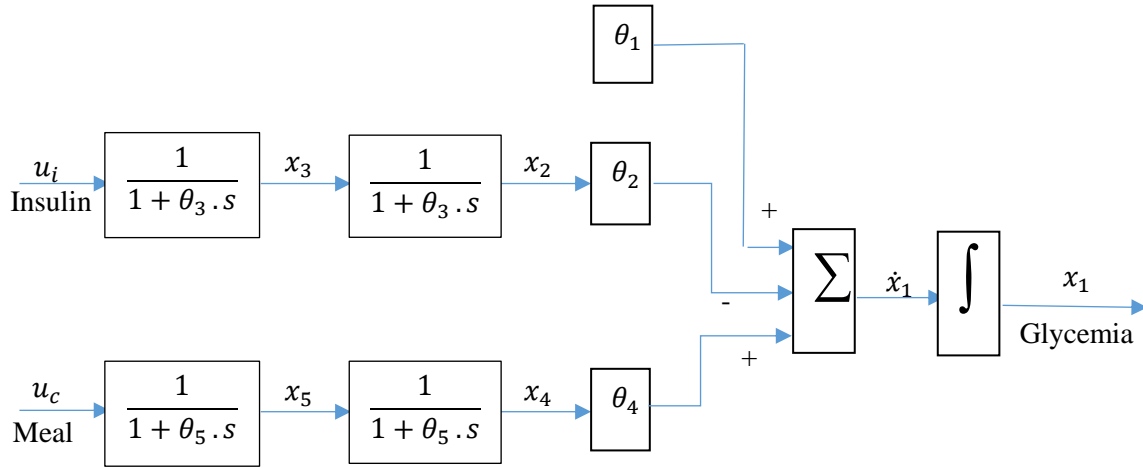


Fig. 3 The Magdelaine's glucose-insulin dynamics structure

The ordinary differential equations are given by:

$$\begin{cases} \dot{x}_1(t) = -\theta_2 x_2(t) + \theta_4 x_4(t) + \theta_1 \\ \dot{x}_2(t) = -\frac{1}{\theta_3} x_2(t) + \frac{1}{\theta_3} x_3(t) \\ \dot{x}_3(t) = -\frac{1}{\theta_3} x_3(t) + \frac{1}{\theta_3} u_i(t) \\ \dot{x}_4(t) = -\frac{1}{\theta_5} x_4(t) + \frac{1}{\theta_5} x_5(t) \\ \dot{x}_5(t) = -\frac{1}{\theta_5} x_5(t) + \frac{1}{\theta_5} u_c(t) \end{cases} \quad (1.1)$$

The model parameters include:

- θ_1 is the difference between the endogenous hepatic glucose production value, and the insulin independent glucose consumption value, [mg/dl/min]. The parameter θ_1 yields hyperglycaemic behaviours of patients with diabetes when all other inputs are zero.
- θ_2 is the insulin sensitivity factor, [mg/dl/U].
- θ_3 and θ_5 are time constants, [min]. The latter refers to the representation of the diffusion time in the insulin compartments and the diffusion time in the digestion compartments, respectively.
- θ_4 is the carbohydrate sensitivity factor, [dl⁻¹].

The state space representation is given by:

$$\begin{pmatrix} \dot{x}_1(t) \\ \dot{x}_2(t) \\ \dot{x}_3(t) \\ \dot{x}_4(t) \\ \dot{x}_5(t) \end{pmatrix} = \begin{pmatrix} 0 & -\theta_2 & 0 & \theta_4 & 0 \\ 0 & -\frac{1}{\theta_3} & \frac{1}{\theta_3} & 0 & 0 \\ 0 & 0 & -\frac{1}{\theta_3} & 0 & 0 \\ 0 & 0 & 0 & -\frac{1}{\theta_5} & \frac{1}{\theta_5} \\ 0 & 0 & 0 & 0 & -\frac{1}{\theta_5} \end{pmatrix} \begin{pmatrix} x_1(t) \\ x_2(t) \\ x_3(t) \\ x_4(t) \\ x_5(t) \end{pmatrix} + \begin{pmatrix} 0 & 0 \\ \frac{1}{\theta_3} & 0 \\ 0 & 0 \\ 0 & \frac{1}{\theta_5} \end{pmatrix} \begin{pmatrix} u_i(t) \\ u_c(t) \end{pmatrix} + \begin{pmatrix} \theta_1 \\ 0 \\ 0 \\ 0 \\ 0 \end{pmatrix} \quad (1.2)$$

$$y(t) = x_1(t)$$

Therefore, we can write;

$$\begin{cases} \dot{X}(t) = A_\theta X(t) + B_\theta U(t) + E_\theta \\ Y(t) = C X(t) \end{cases} \quad (1.3)$$

Here are some important characteristics to note about this model [19]:

1. In Fig. 4, the model displays, as in real life, a single insulin infusion rate U_b known as basal rate, independent from BG, which ensures the equilibrium of value of BG during fasting (u_c, x_5 and $x_4 = 0$).

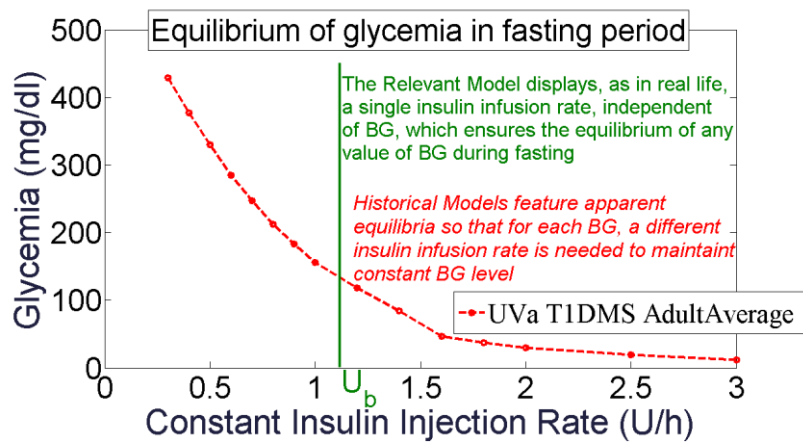


Fig. 4 Equilibrium of glycemia in fasting period (Magdelaine's model in green, UVA/Padova simulator in red) [21]

2. Relevant parameters allow to compute individualized tools for functional insulin therapy:
 - ISF or CF;
 - U_b ;
 - CIR;
 - duration of insulin action (DIA);
 - IOB.

Therefore:

$$ISF = CF = \theta_2 \quad (1.4)$$

$$U_b = \frac{\theta_1}{\theta_2} \quad (1.5)$$

$$CIR = \frac{\theta_2}{\theta_4} \quad (1.6)$$

$$DIA [hours] = \frac{\theta_3 [min]}{12,66} \quad (1.7)$$

3. It is an integrating model (A_θ has an eigen value at zero, which means that it is not stable), it accurately captures the dynamic behavior of the variable in real-life diabetic patients.
4. The model is identifiable and observable.
5. The model gives accurate glucose predictions over 16 hours on average.
6. Glycemic values are limited within the range of 70 mg/dl to 400 mg/dl.

Finally, this model impacts the performance of model-based controllers.

Virtual patients' parameters

The conventional subcutaneous insulin therapy (open-loop therapy) and closed-loop control performance in this work was tested on a virtualized patient cohort consisting of 10 patients, and it is important to note that no modelling of CGM was introduced, therefore, it was assumed that we acquired glucose levels instantaneously without noises. The following Table 1, extracted from [35], displays the θ_i parameters of the 10 patients involved in various *in silico* tests.

Table 1. Flexible insulin therapy model's parameters for the patients

Patient	θ_1 [mg/dl/min]	θ_2 [mg/dl/U]	θ_3 [min]	θ_4 [dl ⁻¹]	θ_5 [min]
1	0.6177	23.4900	60	3.9000	32.5
2	0.5629	45.5214	67	3.7084	36
3	0.4260	51.7588	67	4.0000	37
4	0.3697	16.6632	58	2.8113	35
5	0.4263	47.8641	70	2.4970	40
6	0.9131	41.0474	60	3.5951	40
7	1.1616	36.7843	65	7.3651	53.79
8	0.6653	33.9036	48.39	5.0657	35
9	1.2259	97	60	11.3800	50
10	0.3905	18,7997	73.75	5.3392	55

Also, we aimed to use parameters that mirror real-world scenarios, considering both the patient's condition and the mechanical limitations of the insulin pump. For this purpose, we selected a pump in the market, which offers a basal rate range of 0 to 15 units per hour. We set the minimum bolus size to 0.05 units, while the maximum bolus size was capped at 25 units [38]. The insulin pump and the CGM sampling time was 5 min.

The basal insulin impact on glycemic stability

Before we move on, it's essential to understand that the basal insulin compensates for the natural production of glucose by the liver, maintaining stable blood sugar levels between meals and during sleep [4, 5, 7-12, 14-33, 35-38]. The only true way to determine if the existing basal parameters are functioning correctly is to conduct fasting tests during each phase of the day and night. During a basal test, the only factor that should raise blood sugar levels is the liver, and the only factor that should lower it is basal insulin. All other influences (diet, insulin boluses, physical activity, significant stress, hormonal changes) should be eliminated. An "appropriate" rate of basal insulin infusion is defined as one that maintains blood glucose concentrations at a relatively steady state (< 30 mg/dl change). The adjustments to basal rates were made when blood glucose levels varied by more than 30 mg/dl from the reading taken at the beginning of the test [31].

In order to highlight the characteristics of Magdelaine's model, we performed open-loop simulations using MATLAB-Simulink (R2017a). First, we will assess the impact of the basal insulin value on glycemic stability in the fasting period. To do so, we conduct an open-loop simulation that involves an improperly adjusted basal insulin rate ($\pm 10\%$ of nominal basal insulin). The simulations assume an initial blood glucose level of 160 mg/dl and $U_{b\text{nominal}} = U_b = \frac{\theta_1}{\theta_2}$, as shown in Fig. 5 and Fig. 6.

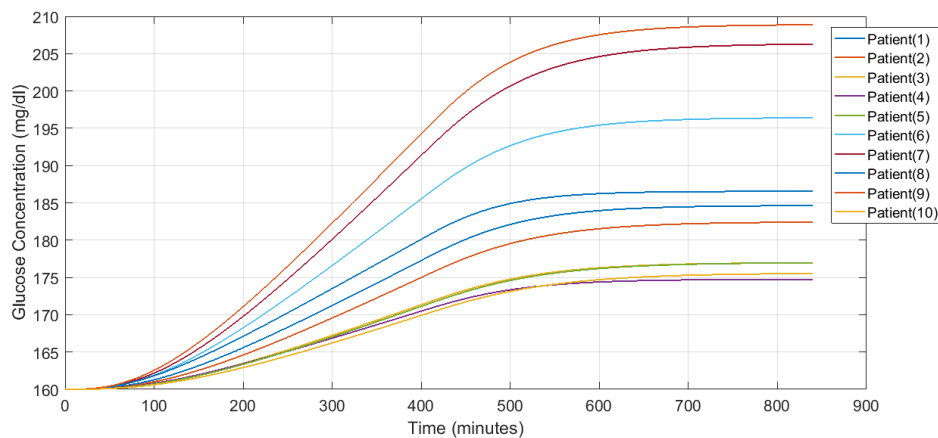


Fig. 5 Glycemia response for basal insulin variations in fasting period, at $t = 0$ min set $U_b = 0.9 \times U_{b\text{nominal}}$, then at $t = 400$ min set $U_b = U_{b\text{nominal}}$

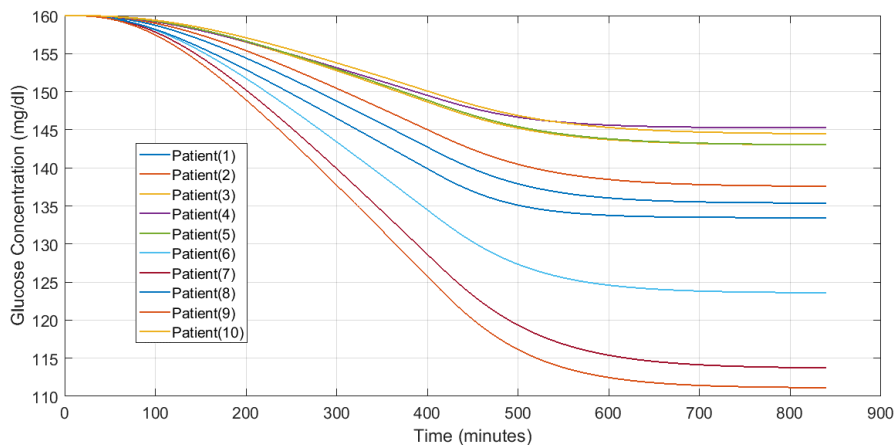


Fig. 6 Glycemia response for basal insulin variations in fasting period, at $t = 0$ min set $U_b = 1.1 \times U_{b\text{nominal}}$, then at $t = 400$ min set $U_b = U_{b\text{nominal}}$

Adjusting basal insulin rate leads to deviations in blood glucose levels, with an increase observed when the rate is lower than the basal rate and a decrease observed when the rate is higher. Following the transient phase, the blood glucose level reaches a stable state when the rate matches the basal rate.

Meals intake without boluses

To simulate the intake of two meals without insulin bolus, each of the 10 patients received 7 g followed by 23.40 g of carbohydrates. Meals can be regarded as impulses, which makes it easier for the user in the sense that it is not necessary to know the duration of the meal but only the amount of carbohydrates in the meal [25]. For simplicity and negligible error, we assumed that the required amount of CHO would be administered over 5 minutes, which corresponds to the system's sampling time. The initial glycemia values were set at 80 mg/dl, and the basal insulin was set as $U_b = \frac{\theta_1}{\theta_2}$.

The analysis of Fig. 7 reveals that, for all patients, the blood sugar level remained stable at the initial value before the first meal, due to a flow rate that matches the basal flow. However, following each meal and after the transient phase, the blood sugar level stabilized at a higher value, contrary to the previous observations made using the UVA/Padova simulator in Fig. 1.

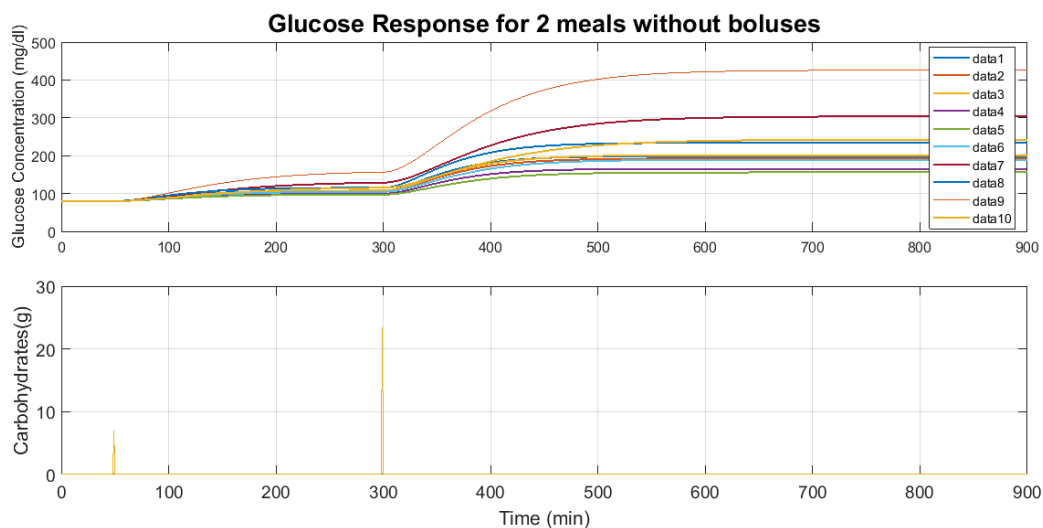


Fig. 7 Glycemia response for 2 meals without boluses

The depicted figure illustrates distinct responses to the same meal intake due to the varying FIT parameters among each patient. In Fig. 8, for instance, patient 9 in Table 1 exhibits a higher sensitivity to carbohydrates, resulting in a post-meal glycaemia level of nearly 420 mg/dl. In contrast, patient 5 displays lower carbohydrate sensitivity, with a post-meal glycaemia level of approximately 155.9 mg/dl. As a result, patient 9 would require more insulin compared to patient 5 to regulate and counterbalance the increase in blood sugar. However, patient 9 has a significantly higher insulin sensitivity factor, twice that of patient 5, necessitating a smaller amount of insulin administration to avoid the risk of hypoglycemic episodes. While this reasoning focuses on only two patients and considers only two parameters (ISF and CIR), it suggests that achieving glycemic regulation, while adhering to specific constraints becomes more complex when dealing with a cohort of ten patients, each with their own distinct set of five parameters.

On the other hand, it's noteworthy that the principle of superposition is upheld. The resulting blood glucose level after separately consuming 7 g of carbohydrates and then 23.40 g is the same as the blood glucose level resulting from ingesting a total of 30.40 g in one go. Let's consider the case of patient 5 with a carbohydrate sensitivity factor of $\theta_4 = 2.49$ mg/dl. For an intake of 7 g of CHO, his blood glucose will increase by 17.48 mg/dl, for 23.40 g it will rise by 58.43 mg/dl, and for 30.40 g it will increase by 75.91 mg/dl. Starting with an initial blood glucose of 80 mg/dl, patient 5 will have a final blood glucose of 155.91 mg/dl ($80 + 17.48 + 58.43 = 155.91$). This outcome is validated by the data presented in Fig. 8.

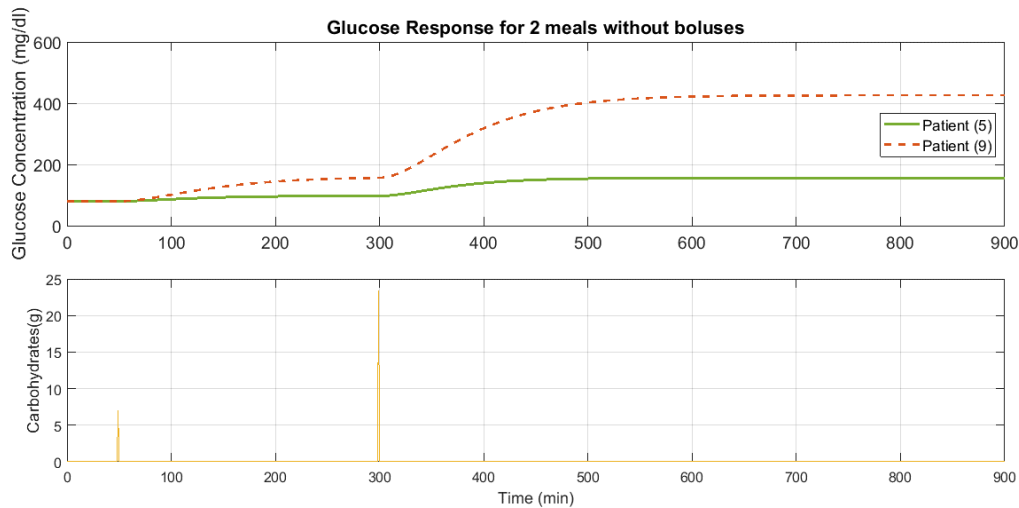


Fig. 8 Two patient's intervariability levels produced with a different response to the same meal intake

Again, let us note that the main objective of basal insulin is not to achieve normal blood glucose levels, but rather to maintain stability over a 24-hour period, with a tolerance of ± 0.30 g/l [4, 5, 7-12, 14-33, 35-38].

Meal's intake accompanied by boluses

To reduce the glucose concentration after a meal, an insulin bolus will now be administered. The bolus insulin dose to be administered should consider both the amount of carbohydrates in the meal and the measured blood glucose level.

The suggested injection as per FIT is U_{Bolus} given by Eq. (1.8) [19], where G is the blood glucose concentration, G_{ref} is the target reference glycaemia, and G_{ref} is set at 110 mg/dl.

$$U_{Bolus} = \frac{CHO(g)}{CIR} + \frac{G - G_{ref}}{ISF} \tag{1.8}$$

In the following sections, all patients were subjected to identical 24-hours meal scenarios.

In the first scenario, as depicted in Fig. 9, each patient received a meal consisting of 7 g of carbohydrates at time $t = 30$ min, followed by 15.80 g at $t = 210$ min, and then 23.40 g at $t = 600$ min, each meal is now accompanied by an appropriate insulin bolus. The initial state vector was $x(0) = [160 \frac{\theta_1}{\theta_2} \frac{\theta_1}{\theta_2} 0 0]$.

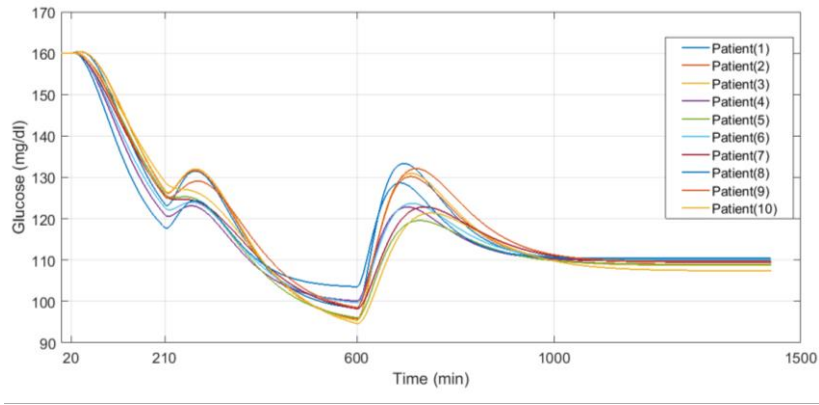


Fig. 9 BG level after meals intake of 7 g, 15.8 g, and 20.4 g, respectively

Let us note that the insulin injection u_i is the sum of the basal rate $U_b = \frac{\theta_1}{\theta_2}$ and the bolus U_{Bolus} . In this case of a 24-hour simulation, u_i will represent the total daily insulin dose (TDI) in units (U) as shown in Table 2.

Table 2. Carbohydrates intake with an appropriate total daily insulin dose

Patient	1	2	3	4	5	6	7	8	9	10
$\Sigma\text{CHO (g)}$	46.20	46.20	46.20	46.20	46.20	46.20	46.20	46.20	46.20	46.20
TDI (U)	47.747	22.730	16.442	42.813	16.331	37.347	56.178	36.667	24.171	45.920

It is clear that the bolus plays a crucial role in eventually bringing the blood glucose levels to the target range. The time it takes to achieve the target blood glucose depends on factors such as the type of insulin used and the amount of carbohydrates consumed, which are closely related to each patient’s individual parameters θ_3 and θ_5 .

It is essential to be aware that the boluses calculated for meal intake using Eq. (1.8) do not consider the insulin on board, which represents the units from previous boluses that are still affecting blood glucose levels. To avoid hypoglycemia, these IOB units need to be subtracted from the calculated injection. Insulin stacking poses a major challenge in the management of intensive insulin therapy for patients with type 1 diabetes.

The insulin on board impact

To evaluate the effect of IOB also known as DIA, which represents how long insulin continues to lower blood glucose levels after it is administered, we will conduct three 24-hour simulation scenarios. In the first and second scenarios, each patient will have two spaced meals with the appropriate bolus insulin. In the third scenario, a third meal will be added between the two previous ones. The initial state vector is $x(0) = [160 \frac{\theta_1}{\theta_2} \frac{\theta_1}{\theta_2} 0 0]$ and $G_{ref} = 110$ mg/dl.

By relying on Eq. (1.7) and Table 1, one can easily calculate the DIA for each patient, as illustrated in Table 3.

Table 3. The duration of insulin action

Patient	1	2	3	4	5	6	7	8	9	10
DIA [h]	4.74	5.29	5.29	4.58	5.53	4.74	5.13	3.82	4.74	5.83

Scenario_1

The patients are depicted receiving two meals with appropriate insulin boluses as shown in Table 4 and Fig. 10a. The first meal, consisting of 7 g of carbohydrates, is given at $t = 0.5$ h, while the second meal, containing 23.40 g of carbohydrates, is administered 9 hours later (9 hours is a larger time than the largest DIA indicated in Table 3).

Table 4. Two meals intake with appropriate insulin boluses and total daily insulin doses (Scenario_1)

Patient	1	2	3	4	5	6	7	8	9	10
CHO (g)	7.00	7.00	7.00	7.00	7.00	7.00	7.00	7.00	7.00	7.00
U_{bolus} (U)	3.291	1.669	1.507	4.182	1.410	1.831	2.761	2.521	1.337	4.648
CHO (g)	23.40	23.40	23.40	23.40	23.40	23.40	23.40	23.40	23.40	23.40
U_{bolus} (U)	3.889	1.911	1.813	3.952	1.226	2.052	4.691	3.497	2.747	6.670
ΣCHO (g)	30.40	30.40	30.40	30.40	30.40	30.40	30.40	30.40	30.40	30.40
TDI (U)	45.073	21.398	15.180	40.104	15.470	35.938	52.957	34.295	22.295	41.249

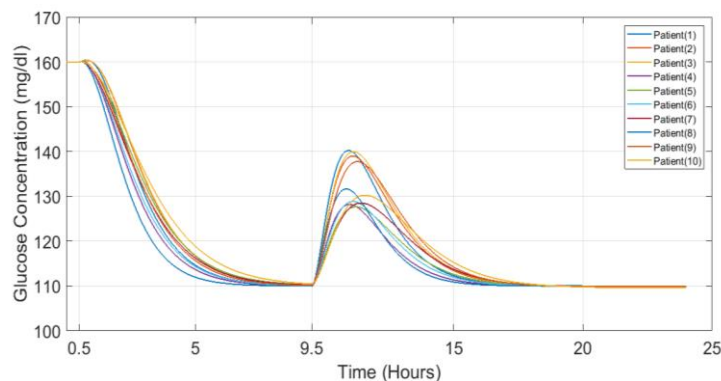
Scenario_2

Similarly, the patients receiving two meals with appropriate insulin boluses as shown in Table 5 and Fig. 10b. The first meal, with 7 g of carbohydrates, is administered at $t = 0.5$ h, while the second meal, consisting of 23.40 g of carbohydrates, is given 6 hours later (6 h correspond to the largest DIA time).

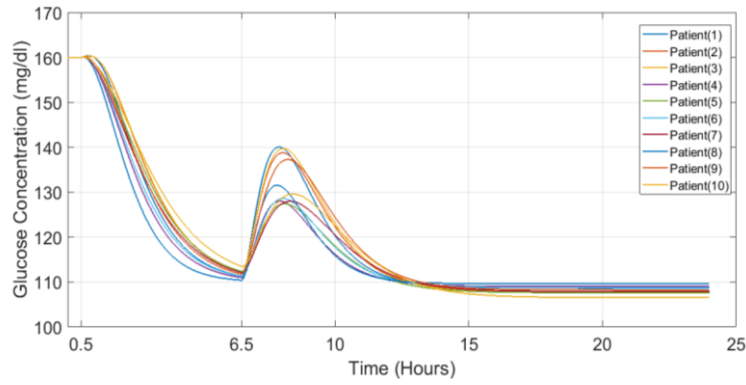
In both scenarios, following an initial transient phase, blood glucose stabilizes and approaches the desired target range (110 mg/dl). Furthermore, it is observed that with a closer spacing of meals, as in the second scenario, a slight increase in TDI is noted.

Table 5. Two meals intake with appropriate insulin boluses (Scenario_2)

Patient	1	2	3	4	5	6	7	8	9	10
CHO (g)	7.00	7.00	7.00	7.00	7.00	7.00	7.00	7.00	7.00	7.00
U_{bolus} (U)	3.291	1.669	1.507	4.182	1.410	1.831	2.761	2.521	1.337	4.648
CHO (g)	23.40	23.40	23.40	23.40	23.40	23.40	23.40	23.40	23.40	23.40
U_{bolus} (U)	3.942	1.955	1.853	4.008	1.271	2.080	4.743	3.508	2.763	6.832
ΣCHO (g)	30.40	30.40	30.40	30.40	30.40	30.40	30.40	30.40	30.40	30.40
TDI (U)	45.125	21.443	15.220	40.160	15.515	35.967	53.009	34.306	22.312	41.412



a) Scenario_1



b) Scenario_2

Fig. 10 BG level for meals intake of 7 g and 20.40 g

Scenario_3

We observe the third scenario where, 3.5 h after the first meal of 7 g of carbohydrates (3.5 h is less than the smallest DIA in Table 3), an additional meal containing 15.80 g of carbohydrates is introduced, while the meal with 23.40 g of carbohydrates remains scheduled for $t = 10$ h. We note that between $t = 7.7$ h and $t = 10$ h, the blood glucose levels tend to stabilize below the desired glucose target (between 97 mg/dl and 105 mg/dl). It is a result of the effects of the two previous boluses. To manage this, the patient must remember to subtract the active insulin units before administering the second bolus or adequately space out the bolus injections. Meals and their appropriate insulin boluses are shown in Table 6 and Fig. 11.

Table 6. Three meals intake with appropriate insulin boluses and TDI (Scenario_3)

Patient	1	2	3	4	5	6	7	8	9	10
CHO (g)	7.00	7.00	7.00	7.00	7.00	7.00	7.00	7.00	7.00	7.00
U_{bolus} (U)	3.291	1.669	1.507	4.182	1.410	1.831	2.761	2.521	1.337	4.648
CHO (g)	15.80	15.80	15.80	15.80	15.80	15.80	15.80	15.80	15.80	15.80
U_{bolus} (U)	3.062	1.580	1.483	3.168	1.096	1.615	3.492	2.520	1.974	5.326
CHO (g)	23.40	23.40	23.40	23.40	23.40	23.40	23.40	23.40	23.40	23.40
U_{bolus} (U)	3.501	1.663	1.592	3.493	0.991	1.845	4.420	3.349	2.649	6.014
Σ CHO (g)	46.20	46.20	46.20	46.20	46.20	46.20	46.20	46.20	46.20	46.20
TDI (U)	47.747	22.730	16.442	42.813	16.331	37.347	56.178	36.667	24.171	45.920

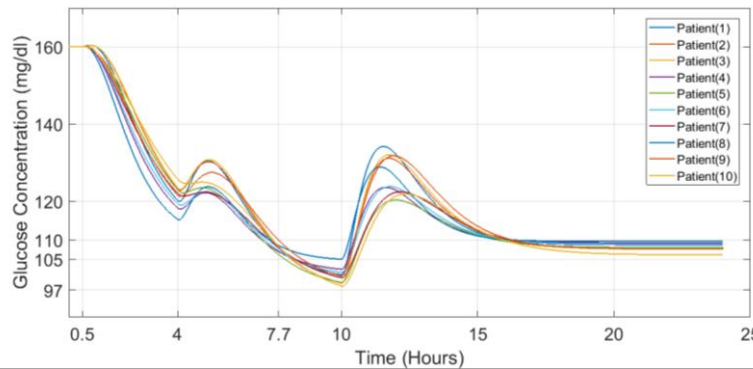


Fig. 11 BG level after 3 meals intake Σ CHO = 46.20 g (Scenario_3)

Scenario_4 and Scenario_5

In the Scenario_4, the same previous scenario is applied, only this time boluses are calculated based on the recommended optimal insulin injections from functional insulin therapy, similar to the bolus wizard method, as follows [19]:

$$U_{bolus} = \frac{CHO(g)}{CIR} + \frac{G-G_{ref}}{ISF} - IOB \quad (1.9)$$

The insulin infusion U_{bolus} consists of three components respectively: a carbohydrate delivery bolus U_{carb} , a correction bolus U_{BG} , and IOB.

IOB can be determined as:

$$IOB = Insulin\ Dose \times \frac{Time\ Remaining}{Insulin\ Duration\ of\ Action} \quad (1.10)$$

Here, the insulin dose represents the last administered bolus, the insulin duration of action (provided in Table 3) refers to the time it takes for an insulin dose to become fully effective and then gradually decrease to zero effect and time remaining is calculated as the difference between DIA and the elapsed time since the insulin was administered (Table 7 and Table 8). Let's note that if we have accurate and measured values for CHO, CIR, ISF, G and IOB, we can calculate the optimal insulin dose.

Table 7. Three meals intake with appropriate insulin boluses and TDI (Scenario_4)

Patient	1	2	3	4	5	6	7	8	9	10
CHO (g)	7.00	7.00	7.00	7.00	7.00	7.00	7.00	7.00	7.00	7.00
U_{bolus} (U)	3.291	1.669	1.507	4.182	1.410	1.831	2.761	2.521	1.337	4.648
CHO (g)	15.80	15.80	15.80	15.80	15.80	15.80	15.80	15.80	15.80	15.80
U_{bolus} (U)	2.201	1.015	0.973	2.182	0.579	1.136	2.615	2.309	1.624	3.469
CHO (g)	23.40	23.40	23.40	23.40	23.40	23.40	23.40	23.40	23.40	23.40
U_{bolus} (U)	4.347	2.211	2.087	4.465	1.490	2.316	5.275	3.559	2.993	7.789
Σ CHO (g)	46.20	46.20	46.20	46.20	46.20	46.20	46.20	46.20	46.20	46.20
TDI (U)	47.732	22.713	16.427	42.799	16.312	37.339	56.156	36.665	24.165	45.837

Table 8. TDI for three meals intake with consideration of the IOB component (Scenario_5)

Patient	1	2	3	4	5	6	7	8	9	10
Σ CHO (g)	138.60	138.60	138.60	138.60	138.60	138.60	138.60	138.60	138.60	138.60
TDI (U)	63.159	30.312	23.635	58.460	21.187	45.474	74.746	50.493	35.043	72.349

In both Fig. 12 and Fig. 13, with the consideration of the IOB component, we note this time that between $t = 7.7$ h and $t = 10$ h, the blood glucose levels tend to stabilize between 112 mg/dl and 134 mg/dl in the 46.20 g case (Scenario_4) and between 115 mg/dl and 170 mg/dl in the case of 138.60 g (Scenario_5), which makes this IOB information crucial for managing blood sugar levels and avoiding potential hypoglycemia.

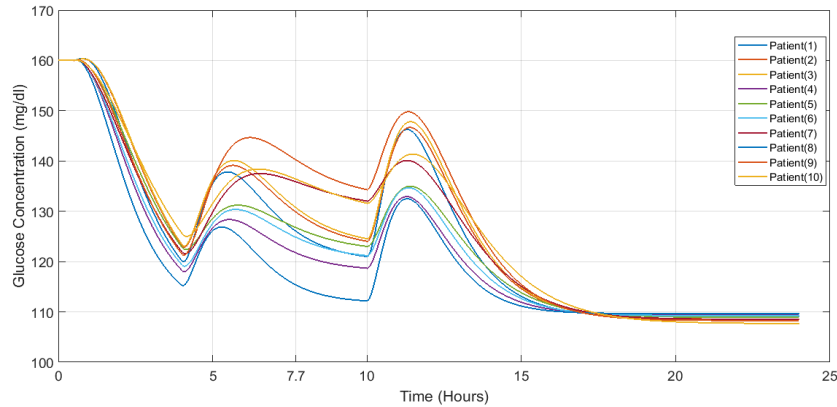


Fig. 12 BG level after 3 meals intake $\sum\text{CHO} = 46.20$ g with the consideration of the IOB component (Scenario_4)

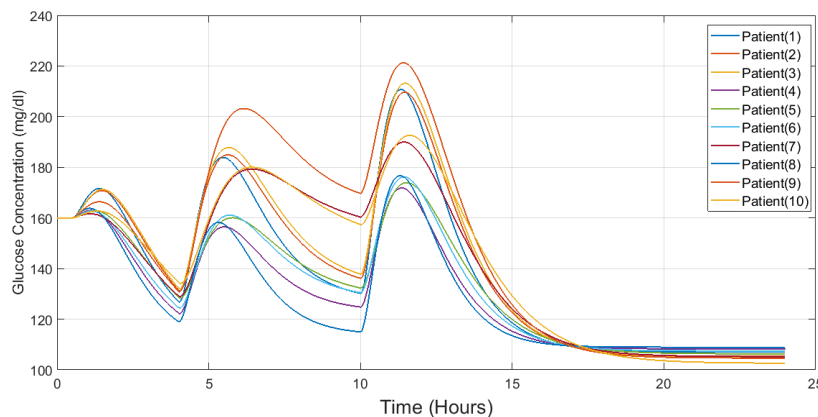


Fig. 13 BG level after 3 meals intake $\sum\text{CHO} = 138.60$ g with the consideration of the IOB component (Scenario_5)

In consideration of the aforementioned, it is necessary to anticipate and react before the glucose concentration rises or falls significantly. To address this issue, future glucose concentrations should be predicted, which is where model predictive control emerges as a solution. By predicting the future glucose concentration, MPC can proactively respond before any substantial change in glucose levels occurs. This predictive capability makes MPC an option for optimizing insulin delivery in closed-loop insulin delivery systems. Also, the optimization formulation can take into account the insulin already administered (IOB), often by imposing constraints to limit the insulin level present at any moment over the prediction horizon [4]. By being proactive rather than reactive, MPC can achieve better glucose control and improve overall diabetes management. Therefore, achieving optimal glycemic control in group of type 1 diabetic patients present a challenge, especially given inherent variability between individuals.

In [30], authors displayed a metamodel (Magdelaine's extend model) for glucose-insulin dynamics that is subject to carbohydrate ingestion and aerobic physical activity and develop a state feedback-based control system for glycemic regulation in type 1 diabetic patients. This control strategy accounted for meal intake and aerobic physical activity. The control algorithm based on the dynamic bolus calculator is proposed by the authors in [35]. Its particular case without exercise, in this case it will be similar to the studied model, can be obtained by setting the physical sensitivity factor to zero. In the next paragraphs, our approach involves using MATLAB-Simulink tools to develop MPC controller aimed at enhancing the time spent within the target glycemic range for all 10 patients.

Model predictive control

MPC is a control strategy that uses a dynamic model of the system to predict its future behaviour and compute an optimal control sequence over a finite time horizon. The control sequence is applied to the system, and the process is repeated at each time step, taking into account new measurements and updating the predictions and control actions.

MPC has the advantage that it uses predictions of the glucose concentration, so it can react before changes occur. The MPC optimization problem has two sets of constraints, a minimum and a maximum value for the calculated insulin infusion rate, and minimum and maximum values for the change of insulin infusion rate between two consecutive time measures. There is a natural minimum of the insulin infusion rate at zero, because insulin cannot be extracted from the blood. The maximum insulin infusion rate should be high in order to ensure the possibility of giving large insulin boluses. The maximum insulin infusion rates and the constraints on change in insulin infusion rate, should be based on the technological limitations of the insulin pump.

The different implementations of MPC share a common overall structure but exhibit variations in the finer aspects. The fundamental structure of MPC schemes is depicted in Fig. 14. The chosen observer utilizes input and output information (u and y , respectively) to compute the estimated state \hat{x} . This estimate is then employed in an optimization process to predict the trajectory of controlled variables, y – over a specific prediction horizon P while adjusting the manipulated variables; u – within a control horizon M that is shorter than the prediction horizon ($M < P$). This predictive step is illustrated in Fig. 15.

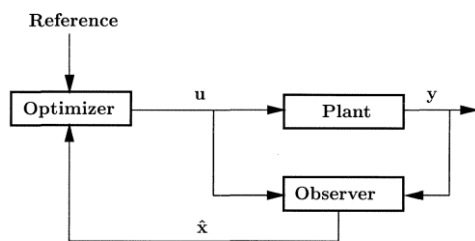


Fig. 14 MPC basic structure [16]

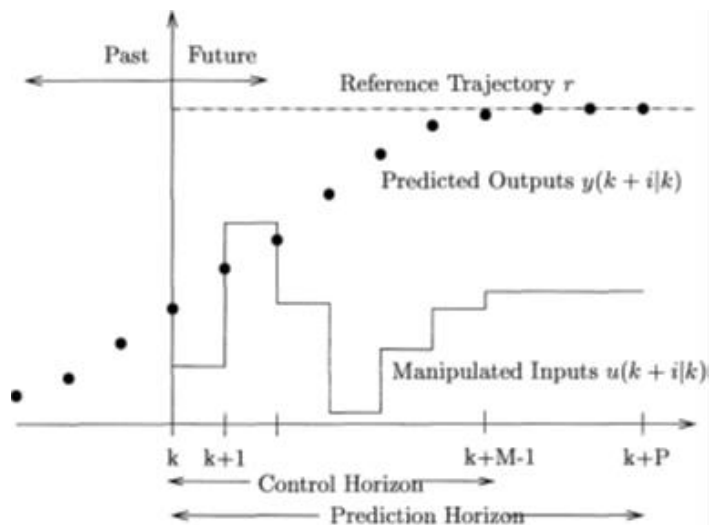


Fig. 15 Optimization problem at time k [12]

At time step k , the optimization algorithm computes the current and future manipulated variable adjustments, $u(k + 1/k), \dots, u(k + M - 1/k)$, in a manner that ensures the anticipated outputs closely follow the designated reference path. The optimizer takes into account any constraints on inputs and outputs by directly incorporating them into the optimization. In the case of linear systems and when employing a linear or quadratic objective function, the resulting optimization problem is linear or quadratic programming, respectively. Among the sequence of control moves only $u(k + 1/k)$, the first move, is executed on the actual system from time step k to $k + 1$. At time step $k + 1$, the measurement $y(k + 1)$ and $u(k + 1/k)$ are utilized by the observer to compute the new estimate $\hat{x}(k + 1)$. The horizons M and P are then shifted one step forward,

and a fresh optimization problem is solved at time step $k+1$, considering the new initial condition $\hat{x}(k+1)$. This process follows the strategy of a moving horizon or receding horizon approach. For practical computational reasons, both the horizons M and P are typically finite values [12].

MATLAB MPC toolbox description

The MPC Toolbox of MATLAB includes application, function, and Simulink blocks for designing and simulating linear and nonlinear MPC controllers. This toolbox allows users to specify plant model parameters, horizons, constraints and weights. Closed-loop simulations can be used to assess controller performance. Controller weights and constraints can be changed during runtime to update output behaviour. In addition to deployable solvers, control designers can employ a custom optimizer from the toolbox. Nonlinear, gain-scheduled and adaptive MPCs can be used to control nonlinear plants [37].

In [36] a model predictive controller uses plant, disturbance, and noise models for prediction and state estimation. In this work, the manipulated variable is the insulin injection rate u_i , the carbohydrate ingestion rate u_c is the measured disturbance and the measured output is the blood glucose concentration x_1 . The MPC controller performs all estimation and optimization calculations using a discrete-time, state-space system with dimensionless input and output variables.

The MPC controller parameters

In this study, the following standard parameters were utilized across all controllers:

- Simple time = 5 minutes.
- Prediction horizon = 80.
- Control horizon = 20.

For the plant models, the nominal value of the manipulated variable is 0.0183 U/min (the mean value of the ten values). Setting the nominal value of the controller slightly different from the nominal value of the plant can have a significant impact on the system's performance and robustness. This adjustment reflects the real-world variations and uncertainties that often exist in the interaction between insulin infusion and glucose response. By aligning the nominal value of the controller with the actual plant conditions, the MPC algorithm becomes more adaptive to the variations encountered during insulin delivery and glucose regulation. This adjustment helps the control system better handle factors like sensor inaccuracies, patient-specific responses, and disturbances. Furthermore, the model-based controller can utilize a separate model distinct from the one used in the simulator [4]. The simulation duration remains constant at 24 hours. Using trial and error, the suitable input constraints are found and displayed in Table 9, we notify that the output is unconstrained:

Table 9. MPC controllers' parameters

MPC controller	Input						Output		
	Constraints				Weights		Constraints		Weight
	Min	Max	RateMin	RateMax	Weight	Rate weight	Min	Max	
Controller 1	0	0.042	-0.004	0.004	0	1	/	/	1
Controller 2	0	0.42	-0.005	0.001	0	5000	/	/	1
Controller 3	0	0.42	-0.05	0.05	0	500	/	/	1

The MPC technique applied here is in linear form with constraints as detailed in [37]. This includes specific aspects such as the cost function, constraints, optimization problem, and QP matrices. In this work, it determines the optimal insulin infusion rate for the next 5 minutes. This decision is based on historical CGM data for the last 100 minutes, past insulin delivery during the same period, and CGM predictions for the next 400 minutes. These predictions are obtained from the model of the system combined with information about future meals. The utilization of an extended prediction horizon, encompassing a longer period, enhances the quality of regulation even in scenarios where predictions may not be entirely accurate [4]. For the model under consideration, the prediction horizon can extend up to 16 hours (i.e. we can extend the prediction horizon up to 192), offering an improvement in control quality. The calculated insulin dose minimizes the disparity between the predicted glucose and the target level. Additionally, it factors in the avoidance of excessive insulin usage. The balance between these two aspects is governed by parameters outlined in Table 9, indicating the “aggressiveness” of the control algorithm, which aligns with the objectives defined by the cost function. Higher values prompt the algorithm to administer more insulin for faster attainment of the target blood glucose, while lower values discourage high insulin doses.

In the following sections of the study, both open-loop and closed-loop simulation conditions for each virtual patient will be similar. This involves maintaining identical initial conditions, i.e. initial state vector $x(0) = [160 \frac{\theta_1}{\theta_2} \frac{\theta_1}{\theta_2} 0 0]$, equivalent quantities of ingested carbohydrates, uniform meal times throughout the simulations at $t = 0.5$ h, $t = 4$ h, $t = 10$ h, respectively, and finally, a $G_{ref} = 110$ mg/dl.

Results and discussion

Optimal conventional treatment scenario

Table 10 and Table 11 displays the results of open-loop simulations, i.e. optimal conventional treatment. Optimal boluses calculated using the Eq. (1.9), which are commonly employed in the daily lives of individuals with type 1 diabetes, are derived from clinical practice. Where, TDI_OL is the open-loop’s TDI. Let’s note that the comparison from MPC and conventional treatment control strategy used in this work suggests that the latter optimizes insulin usage. The average TIR exceed 89.37% for all patients, and notably, with no hypoglycemic episodes. From Table 10, it is evident that for the tenth patient, the third meal of 70.20 g requires a relatively high bolus worth 19.168 units. The essential question to address is as follows: within the framework of MPC regulation, considering the constraints of the insulin pump, can MPC effectively control blood sugar under these conditions, especially when necessitating such insulin dose or more? The response will be unveiled in the subsequent section!

Table 10. OL patient’s TIR, boluses and TDI on one day for 3 meals intake $\sum CHO = 138.60$ g

Patient	1	2	3	4	5	6	7	8	9	10
$\sum CHO$ (g)	138.60	138.60	138.60	138.60	138.60	138.60	138.60	138.60	138.60	138.60
Bolus_1	5.615	2.809	2.589	6.544	2.140	3.057	5.564	4.612	2.979	8.624
Bolus_2	8.601	4.339	4.098	8.755	2.869	4.512	10.018	7.353	5.780	14.779
Bolus_3	11.075	5.372	5.114	11.213	3.372	5.863	13.704	10.252	8.086	19.168
TDI_OL (U)	63.184	30.340	23.661	58.482	21.215	45.488	74.791	50.494	35.056	72.503
TIR (%)	95.56	97.09	96.11	100.00	100.00	100.00	100.00	100.00	97.92	100.00
TBR (%)	0.00	0.00	0.00	0.00	0.00	0.00	0.00	0.00	0.00	0.00
TAR (%)	4.44	2.91	3.89	0.00	0.00	0.00	0.00	0.00	2.08	0.00

Table 11. OL patient’s TIR and TDI on one day for 3 meals intake $\sum\text{CHO} = 184.80 \text{ g}$

Patient	1	2	3	4	5	6	7	8	9	10
$\sum\text{CHO} \text{ (g)}$	184.80	184.80	184.80	184.80	184.80	184.80	184.80	184.80	184.80	184.80
TDI_OL (U)	70.90	34.14	27.27	66.32	23.66	49.56	84.10	57.41	40.50	85.79
TIR (%)	81.47	78.97	77.72	95.14	93.75	93.62	72.52	94.38	63.84	72.80
TBR (%)	0.00	0.00	0.00	0.00	0.00	0.00	0.00	0.00	0.00	0.00
TAR (%)	18.53	21.03	22.28	4.86	6.25	6.38	27.48	5.62	36.16	27.20

The closed-loop control treatment scenario

Table 12 displays the matching of controllers with the appropriate patient. We find that controller 3 can be used to achieve tight performance as it covers a wide range of eight patients with significant variability. It exhibits robust performance even when faced with realistic changes in the process behavior.

Table 12. Matching the controller with the appropriate patient

Patient	1	2	3	4	5	6	7	8	9	10
Controller	Controller 3								X	X

Table 13 and Fig. 16-18 represents the results of the closed-loop simulations based on the MPC controller. These simulations are conducted under the same conditions as those in the open-loop scenario, including initial states, amounts of ingested carbohydrates, and meal timings.

Table 13. Patient’s TIR, TBR, TAR and TDI obtained using the MPC controller for one day with $\sum\text{CHO} = 46.20 \text{ g}$, $\sum\text{CHO} = 92.40 \text{ g}$, $\sum\text{CHO} = 138.60 \text{ g}$, $\sum\text{CHO} = 184.80 \text{ g}$, respectively

Patient	1	2	3	4	5	6	7	8	9	10
$\sum\text{CHO} \text{ (g)}$	46.20	46.20	46.20	46.20	46.20	46.20	46.20	46.20	46.20	46.20
TDI_MPC (U)	48.645	23.150	16.830	43.715	16.595	37.855	57.260	37.500	24.700	46.950
TIR_MPC (%)	100.00	100.00	100.00	100.00	100.00	100.00	100.00	100.00	100.00	100.00
TBR_MPC (%)	0.00	0.00	0.00	0.00	0.00	0.00	0.00	0.00	0.00	0.00
TAR_MPC (%)	0.00	0.00	0.00	0.00	0.00	0.00	0.00	0.00	0.00	0.00
Patient	1	2	3	4	5	6	7	8	9	10
$\sum\text{CHO} \text{ (g)}$	92.40	92.40	92.40	92.40	92.40	92.40	92.40	92.40	92.40	92.40
TDI_MPC (U)	57.166	27.333	20.797	52.378	19.274	42.352	67.540	45.170	30.790	62.077
TIR_MPC (%)	88.24	92.73	92.73	92.73	100.00	93.08	88.24	87.54	85.81	90.31
TBR_MPC (%)	0.00	0.00	0.00	0.00	0.00	0.00	0.00	0.00	6.57	0.00
TAR_MPC (%)	11.76	7.27	7.27	7.27	0.00	6.92	11.76	12.46	7.61	9.69
Patient	1	2	3	4	5	6	7	8	9	10
$\sum\text{CHO} \text{ (g)}$	138.6	138.6	138.6	138.6	138.6	138.6	138.6	138.6	138.6	138.6
TDI_MPC (U)	65.689	31.515	24.764	61.033	21.952	46.848	77.818	52.840	36.738	75.239
TIR_MPC (%)	73.01	80.97	80.62	80.28	90.31	81.66	73.36	75.78	72.66	59.86
TBR_MPC (%)	0.00	0.00	0.00	0.00	0.00	0.00	0.00	0.00	9.34	13.84
TAR_MPC (%)	26.99	19.03	19.38	19.72	9.69	18.34	26.64	24.22	17.99	26.30
Patient	1	2	3	4	5	6	7	8	9	10
$\sum\text{CHO} \text{ (g)}$	184.80	184.80	184.80	184.80	184.80	184.80	184.80	184.80	184.80	184.80
TDI_MPC (U)	74.21	35.70	28.73	69.71	24.63	51.34	88.10	60.51	42.99	91.42
TIR_MPC (%)	64.71	71.63	73.70	67.47	80.62	72.32	64.71	65.05	59.52	45.33
TBR_MPC (%)	0.00	0.00	0.00	0.00	0.00	0.00	0.00	0.00	19.03	19.38
TAR_MPC (%)	35.29	28.37	26.30	32.53	19.38	27.68	35.29	34.95	21.45	35.29

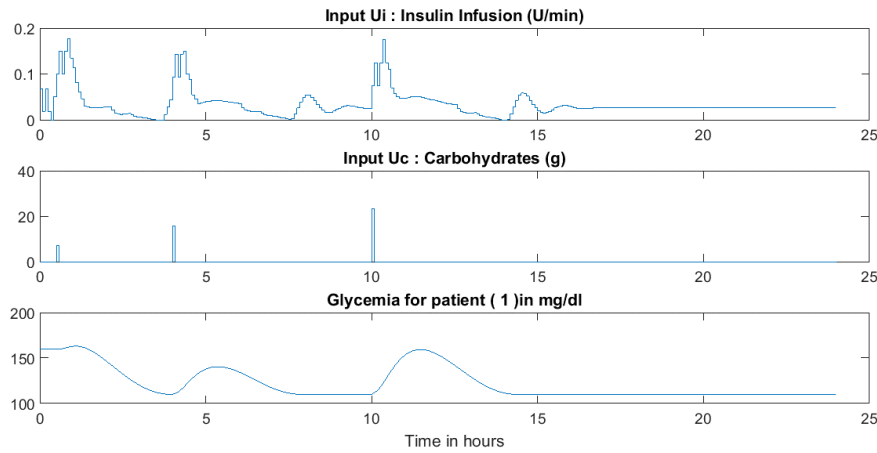


Fig 16. Insulin infusion, CHO intake and glycemia response for patient 1 obtained by using MPC controller ($\sum\text{CHO} = 46.20$ g)

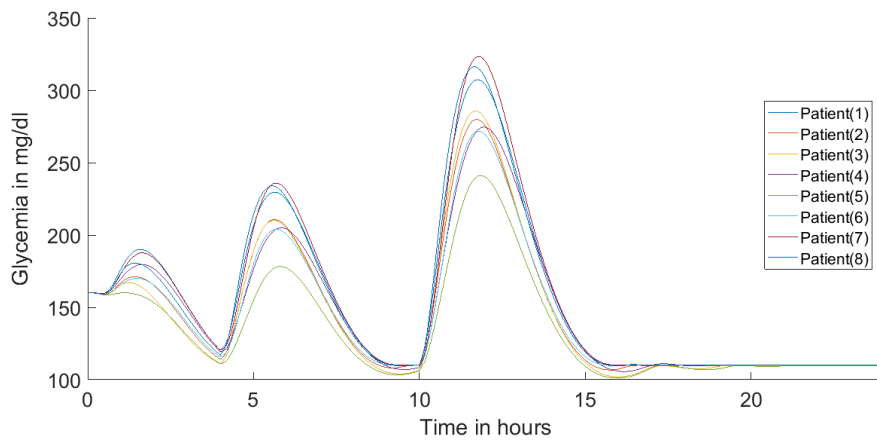


Fig 17. Glycemia response of the first 8 virtual patients obtained by using the MPC controller. The scenario presented here included 3 meals ($\sum\text{CHO} = 138.60$ g) on one day.

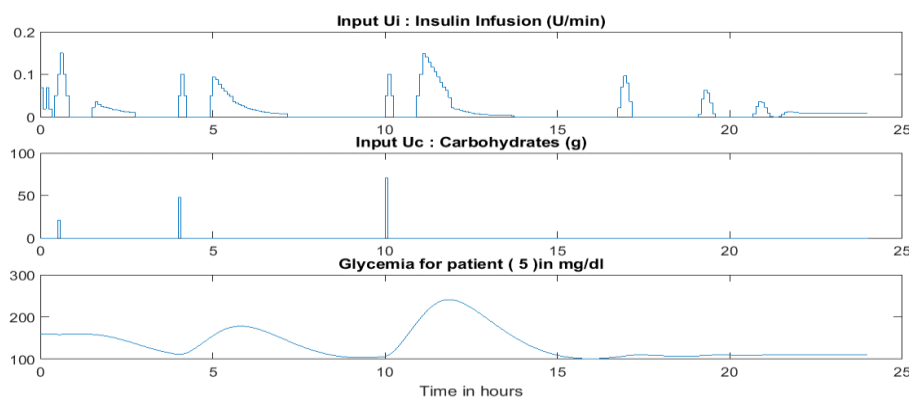


Fig 18. Insulin infusion, CHO intake and glycemia response for patient 5 obtained by using MPC controller ($\sum\text{CHO} = 138.60$ g)

Closed-loop control treatment scenario incorporating glucose measurement delay

In AID systems, there is a well-known delay between the actual plasma glucose concentration and the glucose concentration measured in the interstitial fluid where the CGM sensor is located. Under normal usage conditions of the device and except in certain situations [7]:

- When the sugar level is stable, the interstitial glucose level is equal to the blood glucose level.
- When the sugar level increases (after a meal containing carbohydrates, for example), the interstitial glucose level is lower than the blood glucose level. This results in a delay in the rise of interstitial glucose.
- Conversely, when the sugar level decreases, the interstitial glucose level is higher than the blood glucose level. This results in a delay in the decrease of interstitial glucose.

To allow the interstitial glucose to reach the same level as capillary blood glucose, it takes between 4 to 15 minutes, depending on the person [7, 8, 25].

The Eq. (1.11) models the time delay between blood glucose and interstitial glucose, accounting for the observed delay in changes in glucose concentration across different compartments of the body.

$$\dot{G}_i(t) = \frac{G_b(t) - G_i(t)}{\tau} \quad (1.11)$$

where, $G_b(t)$ is blood glucose concentration (glycemia), [mg/dl]; $G_i(t)$ is interstitial glucose concentration, [mg/dl]; τ is time constant for the delay between blood glucose and interstitial glucose, [min].

This approach simplifies the representation of glucose transport dynamics between blood and interstitial fluid, in line with the mentioned observations.

To account for the time delay between the plasma glucose concentration and its subcutaneous measurement, we can introduce an additional state variable $x_6(t)$, [mg/dl], to represent the subcutaneous glucose concentration. This state will be linked to the plasma glucose concentration $x_1(t)$ through a first-order differential equation that includes the time constant τ , representing the delay.

The equations will be updated to include the dynamics of $x_6(t)$:

$$\begin{cases} \dot{x}_1(t) = -\theta_2 x_2(t) + \theta_4 x_4(t) + \theta_1 \\ \dot{x}_2(t) = -\frac{1}{\theta_3} x_2(t) + \frac{1}{\theta_3} x_3(t) \\ \dot{x}_3(t) = -\frac{1}{\theta_3} x_3(t) + \frac{1}{\theta_3} u_i(t) \\ \dot{x}_4(t) = -\frac{1}{\theta_5} x_4(t) + \frac{1}{\theta_5} x_5(t) \\ \dot{x}_5(t) = -\frac{1}{\theta_5} x_5(t) + \frac{1}{\theta_5} u_c(t) \\ \dot{x}_6(t) = \frac{x_1(t) - x_6(t)}{\tau} \end{cases} \quad (1.12)$$

By adding the differential equation for $x_6(t)$, the modified model now explicitly accounts for the time delay between plasma glucose concentration and its subcutaneous measurement. This enhancement ensures that the model captures the delay effect, making it more accurate and aligned with physiological processes.

Estimation of time delay τ between plasma glucose and subcutaneous measurements based on digestion time constant ($\theta_5\tau$)

To compute the time delay τ for an individual, several approaches typically involve fitting a model to observed data. However, in this work, in the absence of specific data, we can estimate the time delay τ by considering the relationship between the Magdelaine’s model times constants and the physiological processes they represent. Since θ_5 represents the time constant for the digestion subsystem, it might be directly related to τ . For an approximation, we can use the known range of τ (5 to 15 minutes) and try to relate it to $\theta_5\tau$. For example, in the seventh patient’s case, given that θ_5 is 53.79 minutes, we can hypothesize a possible relationship where τ is a fraction of $\theta_5\tau$, since the delay in interstitial glucose levels is generally shorter than the digestion time constant. One simple approach could be to use a scaling factor to estimate τ from $\theta_5\tau$. Considering the typical range of τ (5 to 15 minutes), we can set τ as approximately one-fourth to one-third of $\theta_5\tau$.

$$\tau = \frac{\theta_5}{4} \text{ to } \frac{\theta_5}{3} \tag{1.13}$$

Using $\theta_5 = 53.79$ min: $\tau_{min} \approx \frac{53.79}{4} \approx 13.45$ min and $\tau_{max} \approx \frac{53.79}{3} \approx 17.93$ min.

Given the physiological range of τ (5 to 15 minutes), a value of $\tau \approx 13.45$ min seems reasonable for this patient. This value falls within the typical range and provides a practical estimate based on the digestion time constant. The following Table 14, displays τ_{min} and τ_{max} of the 10 patients involved in various *in silico* tests.

Table 14. Estimated time delay τ between plasma glucose and subcutaneous measurements

Patient	1	2	3	4	5	6	7	8	9	10
θ_5 , [min]	32.50	36.00	37.00	35.00	40.00	40.00	53.79	35.00	50.00	55.00
τ_{min} , [min]	8.13	9.00	9.25	8.75	10.00	10.00	13.45	8.75	12.50	13.75
τ_{max} , [min]	10.83	12.00	12.33	11.67	13.33	13.33	17.93	11.67	16.67	18.33

Tables 15, 16, 17 (along with Figs. 16-18), presents the results of closed-loop simulations using the same MPC controller. These simulations incorporate three different glucose measurement delays: $\tau = 6.0$ min, $\tau = 8.5$ min, and $\tau = 11.0$ min, respectively. All simulations are conducted under the same conditions as those in the previous scenario.

Table 15. Patient’s TIR, TBR, TAR and TDI obtained using the MPC controller for one day with $\sum\text{CHO} = 46.20$ g, $\sum\text{CHO} = 92.40$ g, $\sum\text{CHO} = 138.60$ g and $\sum\text{CHO} = 184.80$ g, respectively, incorporating a glucose measurement delay of $\tau = 6$ min

Patient	1	2	3	4	5	6	7	8	9	10
$\sum\text{CHO}$ (g)	46.20	46.20	46.20	46.20	46.20	46.20	46.20	46.20	46.20	46.20
TDI_MPC (U)	48.871	24.724	16.059	42.821	15.774	39.243	58.076	38.648	27.088	46.176
TIR_MPC (%)	100.00	100.00	100.00	100.00	100.00	100.00	100.00	100.00	66.09	100.00
TBR_MPC (%)	0.00	0.00	0.00	0.00	0.00	0.00	0.00	0.00	33.91	0.00

TAR_MPC(%)	0.00	0.00	0.00	0.00	0.00	0.00	0.00	0.00	0.00	0.00
Patient	1	2	3	4	5	6	7	8	9	10
Σ CHO (g)	92.40	92.40	92.40	92.40	92.40	92.40	92.40	92.40	92.40	92.40
TDI_MPC (U)	56.604	28.367	20.850	52.988	19.248	42.357	66.916	44.822	30.069	59.984
TIR_MPC (%)	90.31	94.81	95.50	93.43	100.00	96.89	86.16	92.39	40.48	78.89
TBR_MPC(%)	0.00	0.00	0.00	0.00	0.00	0.00	0.00	0.00	56.40	10.03
TAR_MPC(%)	9.69	5.19	4.50	6.57	0.00	3.11	13.84	7.61	3.11	11.07
Patient	1	2	3	4	5	6	7	8	9	10
Σ CHO (g)	138.6	138.6	138.6	138.6	138.6	138.6	138.6	138.6	138.6	138.6
TDI_MPC (U)	66.143	33.118	25.291	60.050	22.550	47.988	78.560	53.258	36.613	76.928
TIR_MPC (%)	74.05	80.62	84.08	77.16	91.00	80.28	71.28	75.43	23.53	54.67
TBR_MPC(%)	0.00	0.00	0.00	0.00	0.00	0.00	0.00	0.00	68.17	19.03
TAR_MPC(%)	25.95	19.38	15.92	22.84	9.00	19.72	28.72	24.57	8.30	26.30
Patient	1	2	3	4	5	6	7	8	9	10
Σ CHO (g)	184.80	184.80	184.80	184.80	184.80	184.80	184.80	184.80	184.80	184.80
TDI_MPC (U)	75.140	34.797	29.592	69.398	25.531	52.805	88.992	61.346	42.929	93.438
TIR_MPC (%)	65.74	70.93	72.66	67.82	80.97	71.63	63.67	67.82	24.91	36.68
TBR_MPC(%)	0.00	0.00	0.00	0.00	0.00	0.00	0.00	0.00	64.01	28.72
TAR_MPC(%)	34.26	29.07	27.34	32.18	19.03	28.37	36.33	32.18	11.07	34.60

Table 16. Patient’s TIR, TBR, TAR, and TDI obtained using the MPC controller for one day with Σ CHO = 46.20 g, Σ CHO = 92.40 g, Σ CHO = 138.60 g, and Σ CHO = 184.80 g, respectively, incorporating a glucose measurement delay of $\tau = 8.5$ min

Patient	1	2	3	4	5	6	7	8	9	10
Σ CHO (g)	46.20	46.20	46.20	46.20	46.20	46.20	46.20	46.20	46.20	46.20
TDI_MPC (U)	50.148	23.525	16.928	44.970	16.720	39.622	56.380	37.120	25.287	47.899
TIR_MPC (%)	100.00	100.00	86.51	100.00	94.12	100.00	100.00	100.00	40.48	100.00
TBR_MPC (%)	0.00	0.00	13.49	0.00	5.88	0.00	0.00	0.00	59.52	0.00
TAR_MPC (%)	0.00	0.00	0.00	0.00	0.00	0.00	0.00	0.00	0.00	0.00
Patient	1	2	3	4	5	6	7	8	9	10
Σ CHO (g)	92.40	92.40	92.40	92.40	92.40	92.40	92.40	92.40	92.40	92.40
TDI_MPC (U)	56.727	26.341	21.486	51.653	19.888	41.305	69.244	46.494	30.918	60.814
TIR_MPC (%)	86.16	95.16	91.00	94.46	97.58	100.00	83.74	89.62	22.84	75.78
TBR_MPC (%)	0.00	0.00	5.54	0.00	2.42	0.00	0.00	0.00	74.05	13.15
TAR_MPC (%)	13.84	4.84	3.46	5.54	0.00	0.00	16.26	10.38	3.11	11.07
Patient	1	2	3	4	5	6	7	8	9	10
Σ CHO (g)	138.6	138.6	138.6	138.6	138.6	138.6	138.6	138.6	138.6	138.6
TDI_MPC (U)	66.308	31.021	26.029	61.629	23.259	47.482	76.256	52.834	38.494	77.829
TIR_MPC (%)	73.01	83.74	86.51	77.85	91.35	80.97	71.63	73.70	19.38	51.90
TBR_MPC (%)	0.00	0.00	0.69	0.00	0.00	0.00	0.00	0.00	73.36	22.84
TAR_MPC (%)	26.99	16.26	12.80	22.15	8.65	19.03	28.37	26.30	7.27	25.26
Patient	1	2	3	4	5	6	7	8	9	10
Σ CHO (g)	184.80	184.80	184.80	184.80	184.80	184.80	184.80	184.80	184.80	184.80
TDI_MPC (U)	75.504	35.732	30.114	71.083	26.236	52.802	87.324	60.934	41.948	93.256
TIR_MPC (%)	65.74	72.66	73.36	68.86	80.97	72.66	64.71	66.44	12.46	34.60
TBR_MPC(%)	0.00	0.00	1.38	0.00	0.00	0.00	0.00	0.00	76.12	31.49
TAR_MPC(%)	34.26	27.34	25.26	31.14	19.03	27.34	35.29	33.56	11.42	33.91

Table 17. Patient's TIR, TBR, TAR and TDI obtained using the MPC controller for one day with $\sum\text{CHO} = 46.20$ g, $\sum\text{CHO} = 92.40$ g, $\sum\text{CHO} = 138.60$ g and $\sum\text{CHO} = 184.80$ g, respectively, incorporating a glucose measurement delay of $\tau = 11$ min

Patient	1	2	3	4	5	6	7	8	9	10
$\sum\text{CHO}$ (g)	46.20	46.20	46.20	46.20	46.20	46.20	46.20	46.20	46.20	46.20
TDI_MPC (U)	49.125	24.278	17.148	42.815	16.694	38.743	55.383	37.172	24.501	49.572
TIR_MPC (%)	100.00	97.58	82.70	100.00	90.66	100.00	100.00	100.00	26.99	100.00
TBR_MPC(%)	0.00	2.42	17.30	0.00	9.34	0.00	0.00	0.00	73.01	0.00
TAR_MPC(%)	0.00	0.00	0.00	0.00	0.00	0.00	0.00	0.00	0.00	0.00
Patient	1	2	3	4	5	6	7	8	9	10
$\sum\text{CHO}$ (g)	92.40	92.40	92.40	92.40	92.40	92.40	92.40	92.40	92.40	92.40
TDI_MPC (U)	58.943	27.076	21.712	53.207	20.597	44.052	67.908	46.588	32.464	61.761
TIR_MPC (%)	86.85	89.62	86.51	95.50	95.16	94.12	82.70	88.93	21.80	73.36
TBR_MPC(%)	0.00	7.27	11.42	0.00	4.84	0.00	0.00	0.00	75.09	16.26
TAR_MPC(%)	13.15	3.11	2.08	4.50	0.00	5.88	17.30	11.07	3.11	10.38
Patient	1	2	3	4	5	6	7	8	9	10
$\sum\text{CHO}$ (g)	138.6	138.6	138.6	138.6	138.6	138.6	138.6	138.6	138.6	138.6
TDI_MPC (U)	64.180	31.802	26.354	61.805	20.939	45.462	79.747	53.832	40.003	78.910
TIR_MPC (%)	73.36	83.39	78.55	78.20	80.28	82.35	73.01	75.78	16.26	46.71
TBR_MPC(%)	0.00	4.50	9.34	0.00	11.76	0.00	0.00	0.00	76.47	28.72
TAR_MPC(%)	26.64	12.11	12.11	21.80	7.96	17.65	26.99	24.22	7.27	24.57
Patient	1	2	3	4	5	6	7	8	9	10
$\sum\text{CHO}$ (g)	184.80	184.80	184.80	184.80	184.80	184.80	184.80	184.80	184.80	184.80
TDI_MPC (U)	73.552	36.033	27.987	68.202	23.992	50.560	89.822	59.566	42.157	89.593
TIR_MPC (%)	66.78	70.24	62.63	69.55	70.93	73.36	66.09	67.82	12.11	31.83
TBR_MPC(%)	0.00	4.15	14.88	0.00	12.11	0.00	0.00	0.00	78.89	35.29
TAR_MPC(%)	33.22	25.61	22.49	30.45	16.96	26.64	33.91	32.18	9.00	32.87

Challenges and practical implementation of real-time model predictive control

Although MPC provides significant advantages in terms of performance and flexibility, its real-time implementation presents several challenges. Overcoming these challenges requires a combination of advanced algorithms, precise modeling, efficient computation, and robust implementation strategies. The optimization must be solved within a very short time frame (real-time), often in milliseconds. The complexity of solving this problem increases with the length of the prediction horizon, the number of variables, and the number of constraints. High computational load can lead to delays, making it difficult to meet the real-time requirements, especially for fast dynamical systems. Given that our system has a long response time and the model is linear, a practical implementation is highly feasible.

Conclusion

We advocate Magdelaine's model because of both static and dynamic features have indeed reflected the true behavior of individuals with type 1 diabetes. In this model, we have ascertained that equilibrium points align with clinical observations. These equilibrium points are characterized by a singular basal insulin value, ensuring stability across blood glucose levels. It is noteworthy that the primary purpose of basal insulin is not to achieve normal glucose levels but to maintain stability over a 24-hour period. Additionally, this model uniquely allows the representation of functional insulin therapy tools through its parameters, offering capabilities absent in other models.

Closed-loop simulations, initially conducted without considering the time delay between plasma glucose and interstitial glucose concentrations, were performed under challenging conditions, including elevated initial blood glucose levels, substantial carbohydrate intake, and closely spaced meal times, with a controller sampling time of 5 minutes.

The model predictive control algorithm demonstrated remarkable efficacy in glycemic control for 80% of patients, achieving an average time-in-range percentage exceeding 80% with no hypoglycemic episodes. This aligns with the American Diabetes Association's recommendation of spending at least 70% of the time in the target range for effective glycemic control and maintaining an average time spent in hypoglycemia of less than 4%.

In the second phase, we maintained the same controller but included consideration of the time delay. We modeled this delay and estimated its values based on the time constant for digestion, within the range of 5 to 15 minutes. Incorporating a delay of 6 minutes or less maintained the controller's previously achieved performance. However, a delay of 8.5 minutes resulted in a 10% reduction, with 70% of patients achieving an average time-in-range percentage exceeding 80.02% and an acceptable average time-below-range percentage of 2.09%. In the final scenario, with a time delay of 11 minutes, the MPC algorithm showed poor efficacy in glycemic control for 50% of patients, achieving an average time-in-range percentage exceeding 80.45% with no hypoglycemic episodes. This suggests the need to readjust the MPC controller parameters and/or consider alternative approaches, such as using an adaptive MPC, multiple MPC controllers, or other methods.

References

1. American Diabetes Association (2020). 9. Pharmacologic Approaches to Glycemic Treatment: Standards of Medical Care in Diabetes, *Diabetes Care*, 43(Supplement_1), S98-S110.
2. Battelino T., T. Danne, R. M. Bergenstal, S. A. Amiel, et al. (2019). Clinical Targets for Continuous Glucose Monitoring Data Interpretation: Recommendations from the International Consensus on Time in Range, *Diabetes Care*, 42(8), 1593-1603.
3. Benhamou P. Y., C. Garnier, I. Debaty, A. Rueff, et al. (2010). Basal Insulin Dose in 40 Type 1 Diabetic Patients Remains Stable 1 Year after Educational Training in Flexible Insulin Therapy, *Diabetes & Metabolism*, 36(5), 369-374.
4. Bequette B. W. (2013). Algorithms for a Closed-loop Artificial Pancreas: The Case for Model Predictive Control, *Journal of Diabetes Science and Technology*, 7(6), 1632-1643.
5. Bergenstal R. M., S. Garg, S. A. Weinzimer, B. A. Buckingham, et al. (2016). Safety of a Hybrid Closed-loop Insulin Delivery System in Patients with Type 1 Diabetes, *JAMA*, 316(13), 1407-1408.
6. Bolie V. W. (1961). Coefficients of Normal Blood Glucose Regulation, *Journal of Applied Physiology*, 16(5), 783-788.
7. Borot S., P. Y. Benhamou, C. Atlan, E. Bismuth, et al. (2018). Practical Implementation, Education and Interpretation Guidelines for Continuous Glucose Monitoring: A French Position Statement, *Diabetes & Metabolism*, 44(1), 61-72.
8. Boyne M. S., D. M. Silver, J. Kaplan, C. D. Saudek (2003). Timing of Changes in Interstitial and Venous Blood Glucose Measured with a Continuous Subcutaneous Glucose Sensor, *Diabetes*, 52(11), 2790-2794.
9. Brooker G. (2019). *Handbook of Biomechatronics*, Chapter 11 – The Artificial Pancreas, Academic Press.
10. Brown S. A., B. P. Kovatchev, D. Raghinaru, J. W. Lum, et al. (2019). Six-month Randomized, Multicenter Trial of Closed-loop Control in Type 1 Diabetes, *New England Journal of Medicine*, 381(18), 1707-1717.
11. Brusko T. M., H. A. Russ, C. L. Stabler (2021). Strategies for Durable β cell Replacement in Type 1 Diabetes, *Science*, 373(6554), 516-522.
12. De Oliveira S. L. (1996). *Model Predictive Control for Constrained Nonlinear Systems* (No. 6), vdf Hochschulverlag AG.

13. Djouima M., S. Drid, D. Mehdi (2018). Backstepping Glycemic Control of Type 1 Diabetes for Implementation on an Embedded System, *Int J Bioautomation*, 22(2), 117-132.
14. Hernández-Medina A., C. Flores-Gutiérrez, R. Femat (2018). Robustness Properties Preservation in Suboptimal T1DM H_∞ Control: ω -SPR Substitutions, *Optimal Control Applications and Methods*, 39(1), 220-229.
15. Herold K. C., S. L. Bucktrout, X. Wang, B. W. Bode, et al. (2019). Immunomodulatory Activity of Humanized Anti-IL-7R Monoclonal Antibody RN168 in Subjects with Type 1 Diabetes, *JCI Insight*, 4(24), e126054.
16. Holt R. I., J. H. DeVries, A. Hess-Fischl, I. B. Hirsch, et al. (2021). The Management of Type 1 Diabetes in Adults. A Consensus Report by the American Diabetes Association (ADA) and the European Association for the Study of Diabetes (EASD), *Diabetes Care*, 44(11), 2589-2625.
17. Hovorka R. (2006). Continuous Glucose Monitoring and Closed-loop Systems, *Diabetic Medicine*, 23(1), 1-12.
18. Kovács L. (2017). Linear Parameter Varying (LPV) Based Robust Control of Type-I Diabetes Driven for Real Patient Data, *Knowledge-Based Systems*, 122, 199-213.
19. Magdelaine N. (2017). Diabète de Type 1 du Modèle à la Boucle Fermée, PhD Thesis, École Centrale de Nantes. (in French)
20. Magdelaine N., L. Chaillous, I. Guilhem, J. Y. Poirier, et al. (2016). A Relevant Glucose-insulin Model: Validation Using Clinical Data, *Diabetes Technol Ther*, 18, A93.
21. Magdelaine N., L. Chaillous, I. Guilhem, J. Y. Poirier, et al. (2015). A Long-term Model of the Glucose-insulin Dynamics of Type 1 Diabetes, *IEEE Transactions on Biomedical Engineering*, 62(6), 1546-1552.
22. Mehmood S., I. Ahmad, H. Arif, U. E. Ammara, et al. (2020). Artificial Pancreas Control Strategies Used for Type 1 Diabetes Control and Treatment: A Comprehensive Analysis, *Applied System Innovation*, 3(3), 31.
23. Messori M., C. Toffanin, S. Del Favero, G. De Nicolao, et al. (2019). Model Individualization for Artificial Pancreas, *Computer Methods and Programs in Biomedicine*, 171, 133-140.
24. Mohn A., C. Kavan, E. Bourcelot, C. Zimmermann, et al. (2012). Insulinothérapie Fonctionnelle: un Modèle D'approche Éducative pour les Patients Ayant un Diabète de Type 1, *Médecine des Maladies Métaboliques*, 6(6), 469-476. (in French)
25. Nærum M. (2010). Model Predictive Control for Insulin Administration in People with Type 1 Diabetes, Bachelor's Thesis, Technical University of Denmark.
26. Parihar S., P. Shah, R. Sekhar, J. Lagoo (2022). Model Predictive Control and Its Role in Biomedical Therapeutic Automation: A Brief Review, *Appl Syst Innov*, 5(6), 118.
27. Rahmanian F., M. Dehghani, P. Karimaghvae, M. Mohammadi (2019). Glucose Control in Diabetic Patients Considering Daily Real Life Factors, 6th International Conference on Control, Instrumentation and Automation, 1-5.
28. Rahmanian F., M. Dehghani, P. Karimaghvae, M. Mohammadi (2020). Blood Glucose Control in Type 1 Diabetic Rat, Considering Food Intake Effects, 28th Iranian Conference on Electrical Engineering, 1-5.
29. Rashid T. A., M. K. Hassan, K. Fraser (2019). Improvement of Variant Adaptable LSTM Trained with Metaheuristic Algorithms for Healthcare Analysis, *Advanced Classification Techniques for Healthcare Analysis*, 10, 978-1.
30. Scharbarg E., J. Greck, E. Le Carpentier, L. Chaillous, et al. (2022). A Metamodel-based Flexible Insulin Therapy for Type 1 Diabetes Patients Subjected to Aerobic Physical Activity, *Scientific Reports*, 12(1), 8017.

31. Scheiner G., B. A. Boyer (2005). Characteristics of Basal Insulin Requirements by Age and Gender in Type-1 Diabetes Patients Using Insulin Pump Therapy, *Diabetes Research and Clinical Practice*, 69(1), 14-21.
32. Sherr J. L., L. Heinemann, G. A. Fleming, R. M. Bergenstal (2022). Automated Insulin Delivery: Benefits, Challenges, and Recommendations. A Consensus Report of the Joint Diabetes Technology Working Group of the European Association for the Study of Diabetes and the American Diabetes Association, *Diabetes Care*, 45(12), 3058-3074.
33. Trevitt S., S. Simpson, A. Wood (2016). Artificial Pancreas Device Systems for the Closed-loop Control of Type 1 Diabetes: What Systems Are in Development, *Journal of Diabetes Science and Technology*, 10(3), 714-723.
34. Weisman A., J. W. Bai, M. Cardinez, C. K. Kramer, et al. (2017). Effect of Artificial Pancreas Systems on Glycaemic Control in Patients with Type 1 Diabetes: A Systematic Review and Meta-analysis of Outpatient Randomised Controlled Trials, *The Lancet Diabetes & Endocrinology*, 5(7), 501-512.
35. <https://data.mendeley.com/datasets/x796nk5ysd/draft?a=f30ed41b-ca5a-41d5-8f17-37cd40ff836e> (access date 04 March 2025)
36. <http://www.mathworks.com/help/releases/R2017a/mpc/gs/mpc-modeling.html> (access date 04 March 2025)
37. <https://www.mathworks.com/products/model-predictive-control.html>, Model Predictive Control Toolbox. (access date 04 March 2025)
38. https://www.tandemdiabetes.com/docs/default-source/product-documents/t-slim-x2-insulin-pump/aw-1006534_c_user-guide-tslim-x2-control-iq-7-4-3-mmoll-fra-canada-artwork-web.pdf?sfvrsn=6ec313d7_60, Guide D'utilisation de la Pompe à Insuline T:SLIM X2 avec la Technologie Control-IQ, Version du Logiciel: Control-IQ (7.4). Tandem Diabetes Care (access date 04 March 2025)

Amor Hamata, Ph.D. Student

E-mail: a.hamata@univ-batna2.dz



Amor Hamata was born in Batna, Algeria. He graduated from the Electronic Engineering Department at the University of Batna, Algeria, in 1997. In 2018, Hamata obtained his M.Sc. from the same university. Assuming his role as fraud repression inspector within of Trade and Export Promotion Department of his hometown, he is currently pursuing the Ph.D. degree in Automatic Control.

Assoc. Prof. Salim Aissi, Ph.D.

E-mail: s.aissi@univ-batna2.dz



Salim Aissi was born in Batna, Algeria in 1974. He received his M.Sc. and Ph.D. degrees in Electronic Engineering from University of Batna, Algeria, in 2002 and 2010, respectively. Since 2012, he has been an Associate Professor at the Department of Electronics, University of Batna, Algeria. His research interests are the control of doubly fed induction machines, robust and fuzzy control, and renewable energy.



© 2025 by the authors. Licensee Institute of Biophysics and Biomedical Engineering, Bulgarian Academy of Sciences. This article is an open access article distributed under the terms and conditions of the Creative Commons Attribution (CC BY) license (<http://creativecommons.org/licenses/by/4.0/>).